Part-scale mechanical modelling of LPBF including microstructural evolution effects

De Baere, D.; Bayat, M.; Mohanty, S.; Hattel, J. H.

Published in:
I O P Conference Series: Materials Science and Engineering

Link to article, DOI:
10.1088/1757-899X/861/1/012013

Publication date:
2020

Document Version
Publisher's PDF, also known as Version of record

Part-scale mechanical modelling of LPBF including microstructural evolution effects

IOP Conf. Series: Materials Science and Engineering **861** (2020) 012013 doi:10.1088/1757-899X/861/1/012013

Part-scale mechanical modelling of LPBF including microstructural evolution effects

D De Baere, M Bayat, S Mohanty and J H Hattel

Department of Mechanical Engineering, Technical University of Denmark, Produktionstorvet, Building 425, 2800 Kgs. Lyngby, Denmark

E-mail: ddbae@mek.dtu.dk

Abstract. Due to its nature as a layer-by-layer production technique, the stresses and subsequent deformation from laser-based powder bed fusion are different from the ones observed in other manufacturing techniques. Additionally, because of the cyclic heating and cooling, the material undergoes significant microstructural changes during the process. Especially for the material Ti-6Al-4V, this microstructural change is pronounced, since the microstructure changes from β to α+β during the LPBF process. In this work, two models are coupled together in a novel way. First, a reduced-fidelity part-scale thermo-mechanical model will predict the stresses and deformation. This model uses both the meta-layer concept, and flash heating as methods for decreasing the computational cost. Secondly, a Johnson-Mehl-Avrami-Kolmogorov-based non-isothermal microstructural model is implemented as a state variable to estimate the change in phase fraction of the constituting phases. The results show that the part is made up mostly of a mix of α and α' phases, and that the microstructural change only leads to a small change in the residual stress after the LPBF process.

1. Introduction

Metal additive manufacturing (AM), and particularly laser-based powder bed fusion (LPBF) has become an industrially relevant process. However, due to the unique thermal history, certain aspects of the LPBF process are underexplored. In this paper, a part-scale thermo-mechanical model is two-way coupled with a microstructural model, in order to evaluate the effect of the change in microstructure on the change in the stress state.

In LPBF, a part is produced in a layer-by-layer manner. The LPBF machine deposits a thin layer of metal powder on top of a solid build plate. A laser rapidly melts a cross section of the desired part into the powder layer. The machine then lowers the build plate one step, a new layer is deposited and the process repeats. This cycle continues until the part is produced. Due to this layer-by-layer method of production, relatively high stresses and deformations are present in the final part, affecting the geometrical precision of the final part [1].

Thermo-mechanical modelling of LPBF is a research field that receives much attention in literature, which is illustrated with a non-exhaustive selection of recent works. Chen *et al.* [2] developed a model to predict the effect of the scanning pattern on the stresses in a thin plate-like specimen. Zhang *et al.* [3] performed part-scale simulations to investigate the effect of the mesh on the final part. Ganeriwala *et al.* [4] show, using validation with real samples, the strength of numerical models to predict the stresses in LPBF parts. Finally, Gouge *et al.* [5] performed part-scale models for specific beam-like specimens, showing close correlation between the computed and measured stress profiles. Although

some of these models are capable of simulating the LPBF process on a macro scale, none of these to address the effect of the microstructure on the residual stress level.

In addition to the novel mechanical strain field, the rapid heating and cooling leads to non-equilibrium phases occurring in the part. In this work, the material of choice is Ti-6Al-4V. This metal is commonly used for metal AM, has good corrosion and wear resistance, and excellent mechanical properties, at least in part due to its two-phase nature. Both the α and β phase are equilibrium phases in Ti-6Al-4V, as can be seen in the schematic isopleth in figure 1(b). However, due to the rapid heating and cooling they might not be the resultant phases after the LPBF process. The works by Vrancken *et al.* [6] and Yang *et al.* [7] indicates experimentally that the microstructure after the LPBF process is made up of so-called α', a hexagonal closed packed martensitic non-equilibrium phase. This transformation is schematically represented in figure 1(c). As usual for non-equilibrium phases, heating up the part will result in a transformation from α' into the equilibrium fraction of α and β [8].

Modelling of microstructural transformations in Ti-6Al-4V typically starts with the so-called Johnson-Mehl-Avrami-Kolmogorov (JMAK) equation [9]. This equation describes homogeneous nucleation and growth, which accurately predicts the different phase fractions during an isothermal uniform heat treatment. Modifications to this model have been proposed by Murgau *et al.* [10], who modified the model for non-isothermal heat treatments. They divide the heat treatment into small steps, in which the temperature is assumed constant. Salsi *et al.* [11] adapted this model for the metal AM process, to include the effect of rapid cooling, which is a typical consequence of the laser heating. Both of these models include the decomposition of the α' phase into the equilibrium phases.

Each of these microstructural models calculates the overall microstructural composition of the part. However, to couple the microstructural and the mechanical models. Tan *et al.* [12] formulated such a localised model, which allows them to investigate the effect of the transformation from α to β, and from β to α', the former during heating up and the latter while cooling down to room temperature. What they fail to include is the lagging effect that follows from the kinetics of the phase transformation.

The model presented in this paper aims to improve upon the model presented by Tan *et al.* [12], by using a layer-by-layer part-scale model, which includes flash heating, and couple it with the model proposed by Murgau *et al.* [10]. The geometry is a bridge-type part, similar to the one used by Ganeriwala *et al.*[4]. The geometry is shown in figure 1(a).

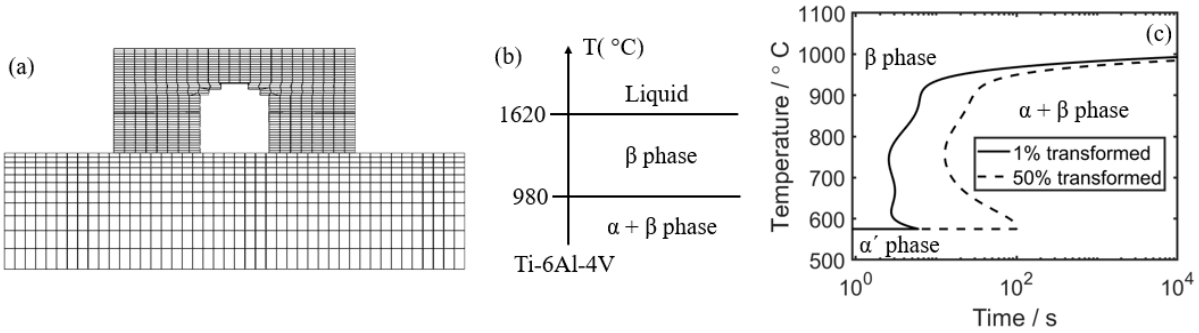

Figure 1. Geometry and material properties of Ti-6Al-4V. (a) The bridge geometry. (b) A schematic isopleth of Ti-6Al-4V, indicating the different equilibrium phases. (c) is a schematic TTT diagram, based on [11] cooling from the β phase.

2. Numerical model

The model that is used to mimic the LPBF process is set up in the commercial suite Abaqus FEA. As the name implies, the discretisation is handled using the finite element discretisation. This implies that the values for the different variables are calculated in the nodes and interpolated between the nodes.

2.1. Governing equations

The model consists of three main components: a thermal part, a mechanical part and a microstructural part. The governing equation for calculating the temperature, *T*, in the model is the traditional transient heat conduction equation:

$$\rho C_p \frac{\partial T}{\partial t} = \left(kT_{,i}\right)_{,i} - \rho \Delta H_{sl} \frac{\partial f_{liq}}{\partial t} + Q_V \tag{1}$$

In equation (1), ρ is the temperature dependent density, C_p is the specific heat capacity, k the thermal conductivity, ΔH_{sl} the latent heat of fusion and f_{liq} the fraction liquid. Q_V is the term representing the heat from the laser. In this work, the flash heating (FH) [13] strategy is used. In FH, a region in the domain, called a meta-layer is heated up at once. Each meta-layer represents a number of real layers. The actual value of the volumetric heat source can be found from the following equation [14]:

$$Q_V = \frac{\alpha P}{H v_{laser} \Delta t_{contact} \delta} \tag{2}$$

This represents the total energy applied to a single real layer. This total energy can be calculated from the effective laser power, represented by the laser power P multiplied by the absorptivity of the powder α. This effective laser power is divided by the time each layer is exposed to it, indicated by the hatch spacing (H), layer thickness (δ) and the laser velocity (v_{laser}). The volumetric heat source can be calculated by including the length of time each ($\Delta t_{\text{contact}}$) meta-layer is exposed to the laser energy.

To obtain the temperature field, each of the aforementioned meta-layers are activated separately, starting from the base plate, until the entire part is activated. The resulting temperature field will have a reduced thermal gradient inside of each meta-layer, but the model gains speed due to a reduction in computational cost.

The basis of the mechanical model is the equation describing static equilibrium:

$$\sigma_{ij,j} = 0 \tag{3}$$

where σ_{ij} is the stress tensor. This is related to the elastic strain via the generalised Hooke's law:

$$\sigma_{ij} = \frac{E}{1+\nu}\left[\frac{1}{2}\left(\delta_{ik}\delta_{jl} + \delta_{il}\delta_{jk}\right) + \frac{\nu}{1-2\nu}\delta_{ij}\delta_{kl}\right]\varepsilon_{kl}^{el} \tag{4}$$

E and ν are the Young's modulus and Poisson coefficient of the material respectively. δ_{ij} is the Kronecker delta, which is one for same, and zero for different indices, and ε_{kl}^{el} is the elastic strain tensor.

An important part of the mechanical model are the plastic and thermal components of the total strain. Finally, because the microstructure is also included in the presented simulations, there is an additional transformation strain component, which plays a role during the simulation. The increments of the elastic, plastic, thermal and transformation strain components are summed to form the total strain increment:

$$\dot{\varepsilon}_{ij}^{\text{total}} = \dot{\varepsilon}_{ij}^{\text{el}} + \dot{\varepsilon}_{ij}^{\text{pl}} + \dot{\varepsilon}_{ij}^{\text{th}} + \dot{\varepsilon}_{ij}^{\text{tr}} \tag{5}$$

Using standard J2 flow theory, the plastic strain increment is given by:

$$\dot{\varepsilon}_{ij}^{pl} = \frac{9}{4\sigma_e^2}\left[\frac{E-E_t}{EE_t}\right]\dot{\sigma}_{kl}s_{ij}s_{kl} \tag{6}$$

The thermal strain increment couples the thermal calculation to the mechanical simulation:

$$\dot{\varepsilon}_{ij}^{\text{th}} = \gamma \delta_{ij} \Delta \dot{T} \tag{7}$$

where γ is the thermal expansion coefficient. Parameters for the mechanical model can be found in [14].

2.2. Microstructural model

As mentioned previously, the temperature, which the part is subjected to during the LPBF process, will affect the composition of the microstructure. In Ti-6Al-4V, there are two major transformations, which will affect the mechanical properties. After the powder has melted, it starts to cool down. Immediately after the part has passed the melting temperature, the entire computational domain is made up of the β phase. This phase is only stable at high temperatures. When the part cools down further, this

β phase decomposes into the equilibrium phase fractions of α and β. This work uses the Castro model [15] to compute these equilibrium fractions:

$$\begin{aligned} X_\beta^{eq} &= 0.925\exp\left(\text{-}0.0085(980\text{-}T)\right)+0.075 \quad \text{for } T<T_\beta \\ X_\beta^{eq} &= 1 \quad \text{for } T>T_\beta \end{aligned} \tag{8}$$

This experimental relation was obtained by cooling slowly from the β phase field, and quenching the bar of the titanium alloy. Experimental observations by Gil Mur *et al.* [8] show that the martensitic phase will decompose into α and β when heated above 400 °C, a process attributed to nucleation and growth of both of these phases.

The JMAK equation for isothermal heat treatments is given by:

$$X_2 = 1 - \exp\left(k_{12}t^{\,n_{12}}\right) \tag{9}$$

where X_2 is the fraction of phase 2, and k_{12} and n_{12} the parameters governing the kinetics of the phase transformation from phase 1 to phase 2.

Although theoretically sufficient, in order to apply equation (9) in the FE framework, which is used for calculating the temperature and stresses during the LPBF process, it needs to be modified. Cahn [16] derived an additivity rule, to take into account partial phase transformations in a small time interval Δt. Leblond and Devaux [17] modified the traditional JMAK equation to include the effect of equilibrium phase fractions, and finally, Murgau *et al.* [10] combined these effects for modelling Ti-6Al-4V. In this work, it is assumed that the calculated phase fractions represent the volume around the FE integration point, and the nodal temperature is representative for the temperature in this finite domain.

After reaching the liquidus temperature of 1620 °C, the entire microstructure is initialised as β. If the cooling rate exceeds 20 °C/s, and the temperature is below the martensitic start temperature (575 °C) the martensite fraction is updated (from the n^{th} numerical iteration to the n+1$^{\text{th}}$):

$$X_{\alpha'}^{\text{n+1}} = X_\beta^{\text{n}} \tag{10}$$

Otherwise, the ordinary α phase forms according to the modified JMAK equations:

$$X_\alpha^{n+1} = \left(1-\exp\left(\text{-}k_{\beta\alpha}\tau^{n_{\beta\alpha}}\right)\right)\left(X_{beta}^{n}+X_{alpha}^{n}\right)X_{\alpha,eq}^{n+1} \tag{11}$$

with τ being the modified time step:

$$\tau = \Delta t + \left[\text{-}\ln\left(1-\frac{X_\alpha^n/X_{\alpha,eq}^{n+1}}{X_\beta^n+X_\alpha^n}\right)\frac{1}{k_{\beta\alpha}}\right]^{\frac{1}{n_{\beta\alpha}}} \tag{12}$$

where Δt is the time step size.

Since the temperature will both increase and decrease during the LPBF process, it is possible that too much of the initial β phase transforms into α according to equations (11) and (12). Therefore, decompositions of the newly formed α phase is necessary. To ensure a smooth evolution of the phase fractions, the decrease of the α phase is [10]:

$$X_\alpha^{n+1} = 1\text{-}X_{\beta,eq}^{n+1} f_{Diss}\sqrt{\Delta\tau} \tag{13}$$

$$\tau = \left(\frac{X_\beta^n}{2.2\times10^{-31}T^{9.89}X_{\beta,eq}^{n+1}}\right)^2 \tag{14}$$

Finally, the dissolution of the martensitic α' phase is discussed. It is known that, when a part is heat treated above 350 °C, but below the β transus temperature, the martensitic phase will decompose into the equilibrium phase fractions of α and β. This transformation is included in the microstructural model as follows:

$$X_{n+1,\alpha'} = \left(1-\exp\left(\text{-}k_{\alpha'}t^{\,n_{\alpha'}}\right)\right)\left(X_{n,\beta}+X_{n,\alpha'}\right) \tag{15}$$

Each of these transformation laws (equations (10), (11) and (13)) are accompanied by complimentary statements ensuring that the sum of the phase fractions is at any point equal to one. The values of the JMAK kinetic parameters are shown in figure 2.

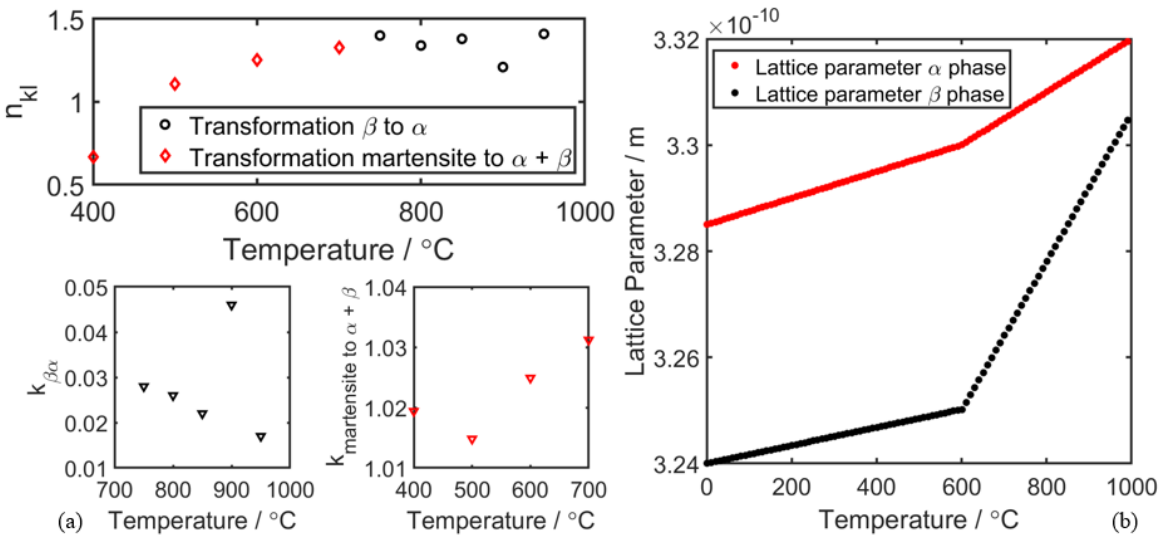

Figure 2. Parameter for the microstructural model. (a) shows the kinetic parameters for phase transformation [8], (b) the lattice parameter of the α and β phases [18].

2.3. Coupling of the microstructural and mechanical models

The microstructural model is clearly coupled to the temperature calculations via the various transformation equations and parameters, which are temperature dependent. Coupling the microstructural model back to the mechanical model is less obvious. This work chooses to implement and additional strain component, namely ε_{ij}^{tr} in equation (5). The transformation strain illustrates the effect of the change in the volume of the different constituting phases. For any phase transformation, the transformation strain can be denoted as [12]:

$$\dot{\varepsilon}_{ij}^{tr} = \delta_{ij} \sum_{kl} \varepsilon_{kl}^{\Delta V} \dot{f}_{kl} \tag{16}$$

where $\varepsilon_{kl}^{\Delta V}$ is the volumetric strain and $\dot{f}_{kl}$ the change in the phase fractions (from k to l). $\varepsilon_{kl}^{\Delta V}$ is calculated from the unit cell volumes of the different phases:

$$\varepsilon_{kl}^{\Delta V} = \frac{\sqrt[3]{V_l} - \sqrt[3]{V_k}}{\sqrt[3]{V_k}} \tag{17}$$

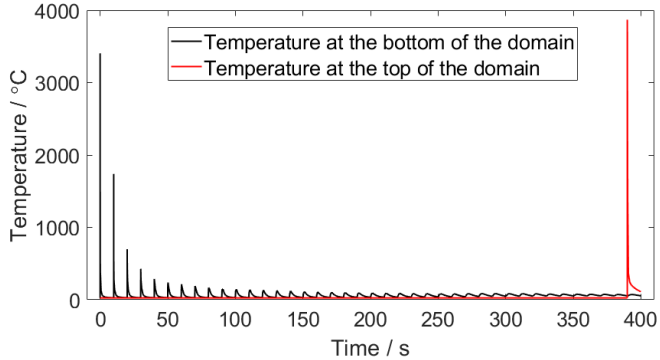

Figure 3. Temperature in the first layer of the simulation and in the final layer.

The different possible transformations are chosen to be α' to α+β, β to α and β to α'. The temperature dependent transformation strain for each of these phases is given in figure 2(b) [18]. Ab initio

computational studies reveal that, for the transformation from martensite to the equilibrium fractions, and expansion of 0.8 percent is expected [19].

2.4. Modelling methodology

The model presented developed in this work uses the flash heating method for mimicking the LPBF process. In each simulation step, one meta-layer, consisting of multiple layers, is activated. The entire meta-layer is subjected to the volumetric heat source, denoted in equation (2). The layer is allowed to cool down, during which the microstructural model continuously updates the phase fractions, based on the temperature in each node and the size of the time steps. Together with the thermal strain, the transformation strain contributes to the stress calculation.

The part is nine millimetre high and divided in 40 meta-layers. The height of each meta-layer is 2.25e-4 millimetre, corresponding to approximately five real layers. To simulate the entire domain of the part within a reasonable amount of time, the mesh is chosen relatively coarse, while at least one layer of elements is present for each meta-layer.

3. Results and discussion

Because FH heats up an entire meta-layer at once, no mayor thermal gradients can be observed inside of each meta-layer. The strongest gradients will exist in the build direction of the part, leading to a stronger variation in stresses and microstructure in this direction. Ssince this model is focussed on part-scale modelling of the process, and this requires reductions in the computational cost, this is an acceptable sacrifice to make, along with the previously chosen coarser mesh.

Figure 3 shows the evolution of the temperature in the first meta-layer of the part, and in the final layer, both on the side of one of the pillars of the bridge. The temperature evolution shows the expected shape, with a single peak in temperature for each deposited layer, when the flash-heating heat flux inputs energy into the domain. The temperature probe at the bottom of the bridge also reveals a significant heating effect of the next layer on the already deposited one, which greatly exceeds the martensite start temperature. When looking at the temperature at the top of the domain, it can be observed that the temperature peak is significantly higher than the one near the build plate. This is most likely due to the heat-sink effect of the build plate being able to conduct more heat away from the part than the part itself.

Figure 4 shows the evolution of the microstructure in the bridge. Figure 4(a) shows the phase fractions on the right of the bridge in the last layer, at the top of the bridge. Figure 4(b) shows the same, but in the first layer, which is located directly on top of the build plate. Observing figure 4(b) reveals that there are three instances where the β fraction jumps one. This corresponds with the first three peaks in temperature at approximately the same points in time in figure 2. The difference in exact position stems from the actual location of the nodal points (where the temperature is calculated) and the integration points (where the phase fractions are defined in Abaqus FEA). However, the temperature only exceeds the β transus temperature for the first two. Moreover, the temperature for these first two peaks is above the melting temperature, indicating that this β fraction actually represents molten material. Since the nodal point is located at the bottom of the domain, the temperature will be lower than at the integration point, which is located slightly higher. Due to the large gradients in this problem, the β-transus temperature is most likely just passed at the phase fraction probe. The first two peaks in the β phase fraction only remain for a very small amount of time, immediately afterwards, the temperature decreases enough that only the equilibrium β fraction remains, while the rest of the domain is comprised of a mix of α and α'. The simulations suggest that, during the initial peaks, a significant amount of α forms, which converts to α' when cooling down further. The third α peak reveals a different behaviour. First of all, β converts significantly slower, due to the high equilibrium fraction at an elevated temperature. This β transforms into α, which is illustrated in the increase of the volume fraction of the latter after 28.7 seconds. Afterwards, the α phase fraction stabilises at 0.448. Since the temperature does not exceed the β-transus temperature at later stages, no large changes in the phase fractions can be found. The amount of α decreases when looking at later layers, but the simulation still shows a significant lack of decomposition of α' into α + β. Rather, the amount of α at the end of the simulation, which is about

44.8 % near the build plate, but around 7 % when halfway up the bridge, is retained α in a martensite matric.

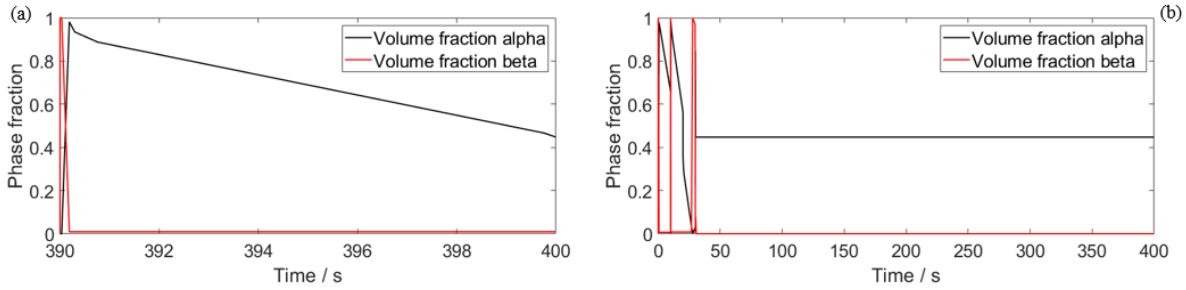

Figure 4. Phase fractions of α and β in the first and last layer. (a) shows the evolution of the β phase fraction in the last layer at the top of the bridge, (b) at the bottom of the bridge, in the first layer.

The phase fraction of β near the top of the domain only undergoes a major change once, due to the deposition of this top layer. On the other hand, understanding of the evolution of the α phase fraction is less straight forward. Figure 4(a) shows that the α phase fraction decreases as time progresses, indicating that the α phase fraction transforms into α'. A possible explanation for this is the order in which the phase fractions are calculated during the simulation: it is possible that the β-phase fraction forms in a time step, if the temperature is high enough to have an appreciable increase of the equilibrium β phase fraction. However, during the same time step, this β fraction will transform into α', due to the high thermal gradient, resulting in this apparent decomposition of α into α'.

Vrancken *et al.* [6] find from light optical microscopy images that the microstructure is entirely martensitic. However, they do not comment on the variation of the microstructure throughout the domain. Salsi *et al.* [11] calculate the α' volume fraction based on X-ray diffraction experiments and find that the volume fraction of a with a similar energy density as the one in this work, varies throughout the part. They find that the martensite volume fraction is around 60 % in the centre of the part. Figure 4(a) and (b) illustrate that the presented model results in final phase fractions which are in between these two values, but are closer to the ones from Salsi *et al.* [11].

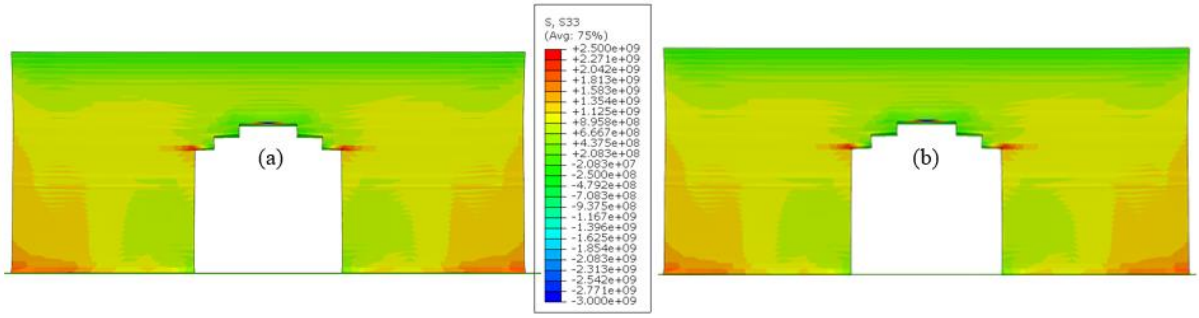

Figure 5. Stress in the bridge. (a) shows the S33 when the microstructural change is simulated, (b) the same when the microstructural change is not included.

Finally, the stress in the bridge is displayed in figure 5, for two cases, one where the microstructural change is accounted for, and one where this was not the case. The second simulation represents the currently most common simulations. Figure 5 shows that there is a minor effect of the phase transformation. As expected from the work by Tan *et al.* [12], the shighest observed stress will increase in the part, however, due to the similarity in the lattice parameter between the α and α', this effect seems rather small. The main differences in the stress contours can be found when looking at the extremities of the bridge-pillars, where the region with the highest stress is slightly larger when the microstructural change is included.The origin of this limited change in stress levels is most likely due to the previously mentioned limited difference between the α and α' lattice parameter: in this work, the change from martensite to the equlibrium phases only results in a 0.8 percent increase of the lattice parameter, based

on the study by Mei *et al.* [19]. Additionally, the microstructural model does not take into account the local grain shape, and the possibility of non-homogeneous grain transformation, which can cause local deviations in the stress profile.

Finally, this paper weighs of the relevance of using the microstructural model. In the present model, with the FH method and JMAK-based microstrucutral model, a relatively fast, part-scale simulaitons are possible, however, the effect of the microstructural change is very small when looking at the final stress profile. Therefore, the additional computational cost is hard to justify.

4. Conclusion

In this work, an LPBF process simulation is expanded to include the microstructural evolution that can take place during the AM of a part in Ti-6Al-4V. The microstructural simulation is based on the well-established JMAK equation, and includes three phases, namely β, α and α'. The conclusions are the following:

- The temperature causes a cyclic transformation from β to α during deposition of a new meta-layer, and the first two layers deposited on top of it. After the heat source is more than three meta-layers away, the microstructure does not change significantly, and a α/α' mixture is predicted by the simulation
- The stress is about five percent higher when including the microstructural change, showing that including the effect of the microstructure on the mechanical stress will improve the simulation of the LPBF process.
- Due to the computational cost and the complexity of the models, including the effect of microstructure can currently only be justified when the exact value of the residual stress and post-process deformation is required.

Acknowledgements

This project has received funding from the European Union's Horizon 2020 research and innovation programme under the Marie Skłodowska-Curie grant agreement No 721383.

References

[1] Kruth J P, Froyen L, Van Vaerenbergh J, Mercelis P, Rombouts M and Lauwers B 2004 *J. Mater. Process. Tech.* **149** 616–22
[2] Chen C, Yin J, Zhu H, Xiao Z, Zhang L and Zeng X 2019 *Int. J. Mach. Tools Manuf.* **145** 103433
[3] Zhang W, Tong M and Harrison N M 2019 *Addit. Manuf.* **28** 610–20
[4] Ganeriwala R K, Strantza M, King W E, Clausen B, Phan T Q, Levine L E, Brown DW and Hodge N E 2019 *Addit. Manuf.* **27** 489–502
[5] Gouge M, Denlinger E, Irwin J, Li C and Michaleris P 2019 *Addit. Manuf.* **29** 100771
[6] Vrancken B, Thijs L, Kruth J P and Van Humbeeck J 2012 *J. Alloys Compd.* **541** 177–85
[7] Yang J, Yu H, Yang H, Li F, Wang Z and Zeng X 2018 *J. Alloys Compd.* **748** 281–90
[8] Gil Mur F X, Rodríguez D and Planell J 1996 *J. Alloys Compd.* **234** 287–9
[9] Avrami M 1939 *J. Chem. Phys.* **7** 1103–12
[10] Murgau C C, Pederson R and Lindgren L E 2012 *Model. Simul. Mater. Sci. Eng.* **20** 055006
[11] Salsi E, Chiumenti M and Cervera M 2018 *Metals* **8** 633
[12] Tan P, Shen F, Li B and Zhou K 2019 *Mater. Des.* **168** 107642
[13] Zaeh M F, Branner G 2010 *Prod. Eng.* **4** 35–45
[14] Bayat M, Klingaa C, De Baere D, Thorborg J, Skat Tiedje N and Hattel JH 2020 *Preprint*
[15] Castro R and Séraphin L 1966 *Mémoires Sci. la Rev. métallurgie.* **58** 1025–58
[16] Cahn J W 1956 *Acta Metall.* **4** 572–5
[17] Leblond J B and Devaux J 1984 *Acta Metall.* **32** 137–46
[18] Elmer J W, Palmer T A, Babu S S and Specht E D 2005 *Mater. Sci. Eng. A* **391** 104–13
[19] Mei W, Sun J and Wen Y 2017 *J. Mater. Res.* **32** 3183–90